Inorg. Chem. **2003**, *42*, 8638–8645

One-Dimensional $CuBr_4^{2-}$ Ion Array and $CuBr_3^-$ Ion Chain Included in the π Conducting Framework Composed of Bis(methylthio)tetrathiafulvalenothioquinone-1,3-dithiocarbonatodithiolemethide Molecules

Takuya Matsumoto,[†] Yohsuke Kamada,[†] Toyonari Sugimoto,*[,†,‡] Toshiji Tada,[†,‡] Satoru Noguchi,[§] Hiroyuki Nakazumi,[§] Takashi Kawakami,[||] Kizashi Yamaguchi,[||] and Motoo Shiro[⊥]

Research Institute for Advanced Science and Technology, Osaka Prefecture University, Osaka 599-8570, Japan, CREST, Japan Science and Technology Corporation, Saitama 332-0012, Japan, Graduate School of Engineering, Osaka Prefecture University, Osaka 599-8531, Japan, Graduate School of Science, Osaka University, Osaka 560-0043, Japan, and Rigaku Corporation, Tokyo 196-8666, Japan

Received March 13, 2003

The reaction of a new donor molecule having a planar but largely bent skeleton, bis(methylthio)tetrathiafulvalenothioquinone-1,3-dithiocarbonatodithiolemethide (**1**), with $CuBr_2$ in CH_3CN/CS_2 afforded a black-colored crystal with a formula of $\mathbf{1}_4$·$CuBr_4$·$2CuBr_3$. In the crystal **1** molecules are one-dimensionally stacked to form half-cut pipelike columns, which are arranged to construct two different shapes of channels included by a one-dimensional array of $CuBr_4^{2-}$ ions and a bibromide-bridged linear chain of $CuBr_3^-$ ions with a square-pyramidal geometry at the Cu atom, $\{CuBr_3^-\}_n$, respectively. The room-temperature electrical conductivity on the single crystal of $\mathbf{1}_4$·$CuBr_4$·$2CuBr_3$ was 2.0×10^{-2} S cm^{-1}, and the temperature dependence of electrical conductivity was semiconducting with a large activation energy of 160 meV. The interactions between the neighboring Cu(II) d spins in the one-dimensional $S = 1/2$ spin systems due to $CuBr_4^{2-}$ ions and $CuBr_3^-$ ions in $\{CuBr_3^-\}_n$ were both antiferromagnetic, and the magnitudes were moderate (Weiss temperature, $\Theta = -18$ K) in the former spin system and fairly large (coupling constant, $J/k_B = -120$ K) in the latter spin system, which was in marked contrast to a moderate and ferromagnetic $\{CuBr_3^-\}_n$ chain in the cyclohexylammonium salt already known.

Introduction

Tetrathiafulvalene (TTF) and tetraselenafulvalene (TSF), and their several substituted derivatives continue to serve as potent donor molecules to produce semi- and superconducting and metallic conducting charge-transfer (CT) salts with several counteranions.[1] In general, in their CT salts the positively charged donor molecules form dimers or one-dimensionally stacked columns, which furthermore are arranged to make up two-dimensionally extended layer structures. Consequently, their crystals are composed of alternate arrangement of two different kinds of layers due to the donor molecules and counteranions. As a matter of course, electrical conduction arises from each of donor molecule layers, while the counteranion layers have only a role as an insulator for dividing the electrical conducting layers into an individual one. However, if the counteranions possess spins, the layers become magnetic, giving rise to a hybrid molecular system with electrical conducting and magnetic layers in an alternate manner.[2] It is much expected that significant interaction between the two different kinds of layers brings about novel physical properties such as giant magnetic resistance (GMR)[3] and furthermore colossal mag-

* To whom correspondence should be addressed. E-mail: toyonari@riast.osakafu-u.ac.jp.
[†] Research Institute for Advanced Science and Technology, Osaka Prefecture University.
[‡] CREST, Japan Science and Technology Corp.
[§] Graduate School of Engineering, Osaka Prefecture University.
[||] Graduate School of Science, Osaka University.
[⊥] Rigaku Corp.

(1) Ishiguro, T.; Yamaji, T.; Saito, G. *Organic Superconductors*; Springer: Berlin, 1998.
(2) Day, P. *Philos. Trans. R. Soc. London, Ser. A* **1985**, *145*, 314.
(3) Baibich, M. N.; Broto, J. M.; Fert, A.; Nguyen Van Dau, F.; Petroff, F.; Etienne, P.; Greuzet, G.; Friederich, A.; Chazelas, J. *Phys. Rev. Lett.* **1988**, *61*, 2472.

10.1021/ic0300971 CCC: $25.00
Published on Web 11/25/2003

netic resistance (CMR) effects,[4] and spin polarization of electric current[5−7] in the molecular systems. With an aim of such an achievement a lot of CT salts with magnetic counteranions using several TTF and TSF derivatives have so far been prepared since the early 1990s. There was undoubtedly fruitful success in the preparation of paramagnetic superconductors,[8−10] metamagnetic superconductors,[11,12] a ferromagnetic metal,[13] and magnetic field-induced ferromagnetic superconductors.[14,15] Nevertheless, significant interaction between the conducting π electrons and the localized d spins was only recognized in the $FeCl_4^-$ and $FeBr_4^-$ salts of bis(ethylenedithio)-substituted TSF (BETS), λ-$(BETS)_2$·$FeCl_4$ and κ-$(BETS)_2$·$FeBr_4$,[16] which exhibited GMR and CMR effects albeit under the conditions of very low temperature (<10 K) and high magnetic field (>10 T).[14,15,17]

In contrast to TTF and TSF derivatives as shown above, a new donor molecule we prepared now, bis(methylthio)-tetrathiafulvalenothioquinone-1,3-dithiocarbonatodithiole-methide (**1**), possesses a high electron-donating ability comparable to those of the parent compound, bis(methylthio)-tetrathiafulvalenothioquinone-1,3-dithiolemethide (**2**)[18] and a familiar dimethylthio-substituted TTF (DMT-TTF),[19] and its whole molecular skeleton is highly planar, but largely bent between the tetrathiafulvalenothioquinone and 1,3-dithiocarbonatodithiole rings. By virtue of such a unique molecular shape, a stacking structure of **1** molecules in the CT salts can be expected to be drastically different from an alternate layer structure in the case of usual donor molecules with a planar and straight molecular skeleton. Very recently, we have demonstrated that the $CuBr_4^{2-}$ salt of a carbonyl analogue of **2** (**3**) has a crystal structure with two different kinds of channels, in each of which neutral copper bromides used in the preparation of the CT salt are included.[20] We now investigated the reaction of **1** with $CuBr_2$ and successfully obtained a new CT salt, $\mathbf{1}_4$·$CuBr_4$·$2CuBr_3$ with such a very unique crystal structure that half-cut pipelike columns composed of **1** molecules are arranged to construct two different shapes of channels included by a one-dimensional array of $CuBr_4^{2-}$ ions and a bibromide-bridged linear chain of $CuBr_3^-$ ions with a square-pyramidal geometry at the Cu atom, $\{CuBr_3^-\}_n$, respectively. Each of the **1**-stacked columns has almost no contact with each other to be essentially one-dimensional, and both of the $CuBr_4^{2-}$ ions and $CuBr_3^-$ ions in $\{CuBr_3^-\}_n$ construct one-dimensional Cu(II) ($S = 1/2$) d spin systems completely isolated from each other. However, the one-dimensional **1**-stacked columns and d spin array or chain are located very closely with each other to bring about significant interaction between them, so that novel electrical conducting and magnetic properties can be expected to be observed.

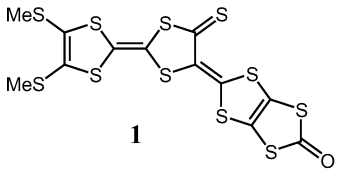

1

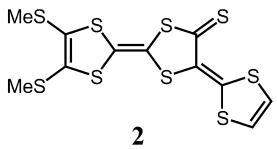

2

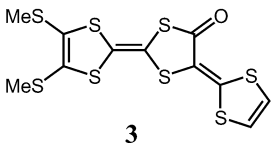

3

Experimental Section

Synthesis of 1 and $\mathbf{1}_4$·$CuBr_4$·$2CuBr_3$. Bis(tetraethylammonium) bis(2,3-bis(methylthio)tetrathiafulvalenyl-6,7-dithiolato)zinc complex[21] (100 mg, 9.6×10^{-3} mmol) was reacted with 5 equiv of 2-(methylthio)-1,3-dithiole-2-oxo-4,5-dithiolanium tetrafluoroborate (156 mg, 4.8×10^{-3} mmol) in THF/DMF (1:1 v/v) at rt (room temperature) under argon, and stirring was carried out for 8 h. After separation of the reaction mixture by column chromatography on silica gel (eluent: CS_2), followed by recrystallization from CS_2/*n*-hexane, **1** was obtained as a black-colored crystal (mp 123−124 °C) in 41% yield. Anal. Calcd for $C_{12}H_6OS_{11}$: C, 27.78; H, 1.17. Found: C, 27.88; H, 1.28. A solution of **1** (2.0 mg, 3.9×10^{-3} mmol) in CS_2 (4 mL) was contacted to a CH_3CN solvent (2 mL), which was further contacted to a solution of $CuBr_2$ (30 mg, 0.13 mmol) in CH_3CN (3 mL).[20] When this three-phase solution was kept at rt for about 1 week, a black-colored crystal, $\mathbf{1}_4$·$CuBr_4$·$2CuBr_3$ (mp > 300 °C), appeared at the interface between the upper two phases. Anal. Calcd for $C_{48}H_{24}O_4S_{44}Cu_3Br_{10}$: C, 18.81; H, 0.79. Found: C, 18.69; H, 0.88.

X-ray Data Collection, Structure Solution, and Refinement. The X-ray diffraction data were collected at 173 and 93 K for **1** and $\mathbf{1}_4$·$CuBr_4$·$2CuBr_3$, respectively, on a Rigaku RAXIS-RAPID imaging plate diffractometer with graphite-monochromated Mo Kα radiation (λ = 0.710 75 Å). The crystallographic data for **1** and

(4) Jin, S.; Tiefel, T. H.; McCormack, M.; Fastnacht, R. A.; Ramesh, R.; Chen, L. H. *Science*, **1994**, *264*, 413.
(5) Prinz, G. A. *Science* **1998**, *282*, 1660.
(6) Ball, P. *Nature* **2000**, *404*, 918.
(7) Ohno, H. *Science* **2001**, *291*, 840.
(8) Graham, A. W.; Kurmoo, M.; Day. P. *J. Chem. Soc., Chem. Commun*. **1995**, 2061.
(9) Kurmoo, M.; Graham, A. W.; Day, P.; Coles, S. J.; Hursthouse, M. B.; Caulfield, J. L.; Singleton, J.; Pratt, F. L.; Hayes, W.; Ducasse, L.; Guionneau, P. *J. Am. Chem. Soc.* **1995**, *117*, 12209.
(10) Martin, L.; Turner, S. S.; Day, P.; Mabbs, F. E.; McInnes, E. J. L. *Chem. Commun.* **1997**, 1367.
(11) Ojima, E.; Fujiwara, H.; Kato, K.; Kobayashi, H.; Tanaka, H.; Kobayashi, A.; Tokumoto, M.; Cassoux, P. *J. Am. Chem. Soc.* **1999**, *121*, 5581.
(12) Fujiwara, H.; Fujiwara, E.; Nakazawa, Y.; Narymbetov, B. Zh.; Kato, K.; Kobayashi, H.; Kobayashi, A.; Tokumoto, M.; Cassoux P. *J. Am. Chem. Soc*. **2001**, *123*, 306.
(13) Coronado, E.; Galán-Mascarós, J. R.; Gómez-Garcia, C. J.; Laukhin, V. *Nature* **2000**, *408*, 447.
(14) Uji, S.; Shinagawa, H.; Terashima, T.; Yakabe, T.; Tokumoto, M.; Kobayashi, A.; Tanaka, H.; Kobayashi, H. *Nature* **2001**, *410*, 908.
(15) Fujiwara, H.; Kobayashi, H.; Fujiwara, E.; Kobayashi, E. *J. Am. Chem. Soc*. **2002**, *124*, 6816.
(16) Kobayashi, H.; Tomita, H.; Naito, T.; Kobayashi, A.; Sakai, F.; Watanabe, T.; Cassoux, P. *J. Am. Chem. Soc*. **1996**, *118*, 368.
(17) Zhang, B.; Tanaka, H.; Fujiwara, H.; Kobayashi, H.; Fujiwara, E.; Kobayashi A. *J. Am. Chem. Soc.* **2002**, *124*, 9982.
(18) Iwamatsu, M.; Kominami, T.; Ueda, K.; Sugimoto, T.; Fujita, H.; Adachi, T. *Chem. Lett.* **1999**, 329.
(19) Inokuchi, H.; Saito, G.; Wu, P.; Seki, K.; Tang, T. B.; Mori, T.; Imaeda, K.; Enoki, T.; Higuchi, Y. Inaka, K.; Yasuoka, N. *Chem. Lett.* **1986**, 1263.
(20) Matsumoto, T.; Kamada, Y.; Sugimoto, T.; Tada, T.; Nakazumi, H.; Kawakami, T.; Yamaguchi, K. *Synth. Met.* **2003**, *135−136*, 575.
(21) Ueda, K.; Yamanoha, M.; Sugimoto, T.; Fujita, H.; Ugawa, A.; Yakushi, K.; Kano, K. *Chem Lett.* **1997**, 461.

Table 1. Crystallographic Date for **1** and $\mathbf{1}_4$·$CuBr_4$·$2CuBr_3$

	1	$\mathbf{1}_4$·$CuBr_4$·$2CuBr_3$
formula	$C_{12}H_6S_{11}O$	$(C_{12}H_6S_{11}O)_4$·$CuBr_4$·$2CuBr_3$
M_r	518.84	3065.04
cryst size (mm)	0.30 × 0.25 × 0.03	0.20 × 0.03 × 0.02
cryst habit	black, platelet	black, needle
cryst syst	triclinic	orthorhombic
space group	$P\bar{1}$	Ibca
a (Å)	8.395(2)	6.949(3)
b (Å)	14.273(4)	38.09(2)
c (Å)	16.517(3)	33.12(1)
α (deg)	91.10(1)	90
β (deg)	103.56(1)	90
γ (deg)	101.68(1)	90
V (Å^3)	1879.5(8)	8767(6)
Z	4	16
temp (K)	173	93
ρ (g cm^{-3})	1.833	2.322
$\mu_{MoK\alpha}$ (cm^{-1})	12.82	64.41
$2\theta_{max}$	55	51
voltage (kV), current (mA)	56, 40	60, 90
scan type	ω	ω
unique data	8468	4088
R_{merge}	0.06	0.14
weighting scheme	$1/\sigma^2(F_o^2)$	$1/\sigma^2(F_o^2)$
resid electron dens (min, max) (e Å^{-3})	−1.42, 1.35	−1.92, 2.12
no. of params refined	433	250
R1[a]	0.058	0.063
wR2[b]	0.082	0.093

[a] $R1 = (\sum||F_o| - |F_c||)/(\sum|F_o|)$. [b] $wR2 = [\sum w(F_o^2 - F_c^2)^2/\sum w(F_o^2)^2]^{1/2}$.

$\mathbf{1}_4$·$CuBr_4$·$2CuBr_3$ are summarized in Table 1. The structures were solved by direct methods (SIR92,[22] SIR97,[23] and DIRDIF94[24]), and refined on F_o^2 with full-matrix least-squares analysis. Calculated positions of the hydrogen atoms [d(C−H) = 0.95 Å] were included in the final calculations. All the calculations were performed by using the teXsan crystallographic software package of the Molecular Structure Corp.[25] For **1** the final cycle of least-squares refinement on F_o^2 for 8468 data and 433 parameters converged to $wR2(F_o^2)$ = 0.082 and R1 = 0.058 for all the data. For $\mathbf{1}_4$·$CuBr_4$·$2CuBr_3$ the final cycle of least-squares refinement on F_o^2 for 4088 data and 250 parameters converged to $wR2(F_o^2)$ = 0.093 and R1 = 0.063 for all the data.

Electrical Conductivity, ESR, and Magnetic Susceptibility Measurements. Electrical conductivity was measured on the single crystal of $\mathbf{1}_4$·$CuBr_4$·$2CuBr_3$ using a four-probe method in the temperature range 113−300 K. The contact to the electrode was performed with gold paste. The ESR spectra of the microcrystals of $\mathbf{1}_4$·$CuBr_4$·$2CuBr_3$ at different temperatures between 3.5 and 300 K were recorded with a frequency of 9.46672 GHz using a Bruker ESP-300E spectrometer. The g value was determined using a gaussmeter. The magnetization at different temperatures between 1.8 and 300 K was measured using the microcrystals of $\mathbf{1}_4$·$CuBr_4$·$2CuBr_3$ under an applied field of 1 kOe with a SQUID magnetometer (MPMS XL, Quantum Design). The magnetic susceptibility (χ_{obs}) was obtained by dividing the magnetization with the applied field used. The paramagnetic susceptibility (χ_p) was obtained by subtracting the diamagnetic contribution calculated by the Pascal method[26] from χ_{obs}.

Results and Discussion

Molecular Structure, Redox Property, and HOMO of 1. The crystal of **1** involves two crystallographically independent molecules (**1a**,**b**). As their molecular structures are shown in Figure 1a,b, both of the molecular skeletons including the two CH_3S S atoms are almost planar: the dihedral angles between rings I and II, between rings II and III, and between rings III and IV are 3.7, 4.0, and 1.5° for **1a** and 3.5, 2.0, and 1.0° for **1b**, respectively. The two CH_3S C atoms are located down from the ring I plane including the two CH_3S S atoms by 0.63 and 1.77 Å for **1a**, while they are up by 0.14 and 1.78 Å for **1b**, respectively. However, the rings I/II and III/IV are largely bent from each other by the angles of 34.0° in **1**a and 33.8° in **1b**. The C═C and C−S bonds in the tetrathiaethylene moiety and the C═S bonds have distances of 1.33−1.34, 1.77, and 1.66−1.67 Å, respectively, and these values are almost the same as those of **2**.[18] The C═O bond distances are 1.20 and 1.21 Å and comparable to those of normal C═O compounds.[27]

In the cyclic voltammogram of **1** measured in DMF two pairs of reversible redox waves were observed, which correspond to electron-transfer processes between **1** and its radical cation and between the radical cation and its dication, respectively. Their redox potentials are +0.63 and +0.76 V vs Ag/AgCl, which are lower by 0.01−0.05 V than those

(22) Altomare, A.; Burlea, M. C.; Gamalli, M.; Cascarano, G. L.; Giacovazzo, C.; Guagliardi, A.; Polidre, G. *J. Appl. Crystallogr*. **1994**, *27*, 435.
(23) Altomare, A.; Burlea, M. C.; Gamalli, M.; Cascarano, G. L.; Giacovazzo, C.; Guagliardi, A.; Moliterni, A. G. G.; Polidre, G.; Spagna, R. *J. Appl. Crystallogr*. **1999**, *32*, 115.
(24) Beurskens, P. T.; Admiraal, G.; Beurskens, G.; Bosman, W. P.; de Gelder, D.; Israel, R.; Smith, J. M. M. *Technical Report of the Crystallography Laboratory*; University of Nijmegen: Nijmegen, The Netherlands, 1994.
(25) *TeXsan, Crystal Structure Analysis Package*; Molecular Structure Corp.: Houston, TX, 1985 and 1992.
(26) König, E. *Landolt-Bornstein, Group II: Atomic and Molecular Physics, Vol. 2, Magnetic Properties of Coordination and Organometallic Transition Metal Compounds*; Springer-Verlag: Berlin, 1966.
(27) Sutton, L. E. *Tables of Interatomic Distances and Configuration in Molecules and Ions*; The Chemical Society Special Publication, No. 11, 18; The Chemical Society: London, 1958, 1965.

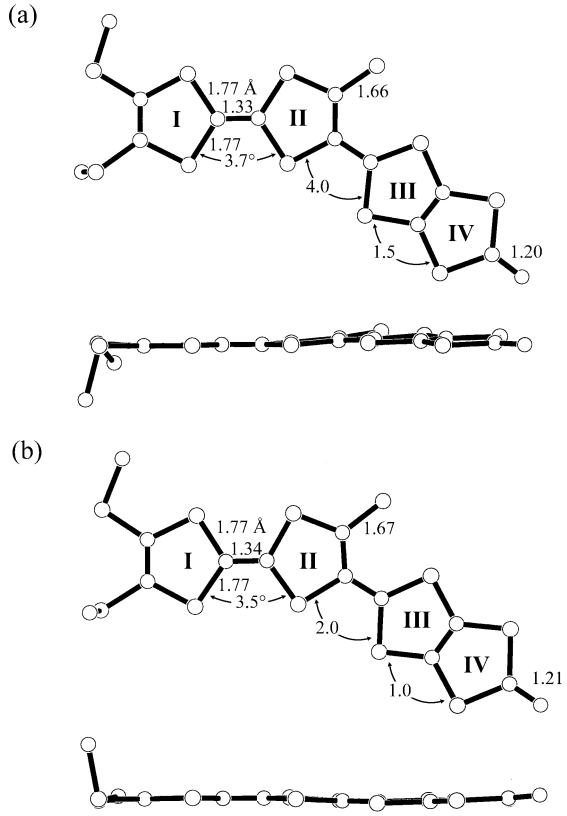

Figure 1. Molecular structures of two crystallographically independent **1** molecules: (a) **1a**; (b) **1b**.

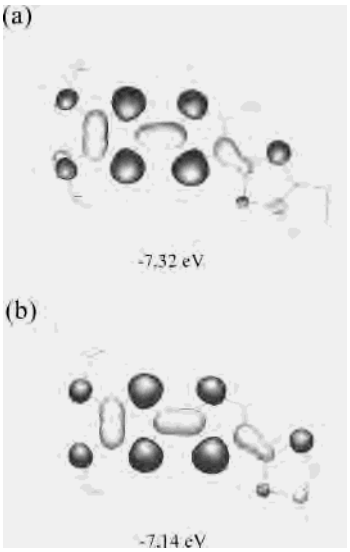

Figure 2. Energies and AO distribution in HOMOs of (a) **1** and (b) **2**.

(+0.64 and +0.80 V) of **2**,[18] while higher by 0.10−0.12 V than those (+0.51 and +0.66 V) of DMT-TTF.[19] In correspondence to the experimental results as above, the MOPAC-MO calculations[28] show that the HOMO of **1** (−7.32 eV) is located at a slightly lower energy level than that of **2** (−7.14 eV). As seen from the atomic orbital (AO) distribution in each of the HOMOs in Figure 2a,b, the AO coefficients are large at the central tetrathiaethylene moiety and moderate at the C═C bond of the I/II ring, at the S atoms

(28) Stewart, J. J. P. *MOPAC 2000*; Fujitsu Limited: Tokyo, 1999.

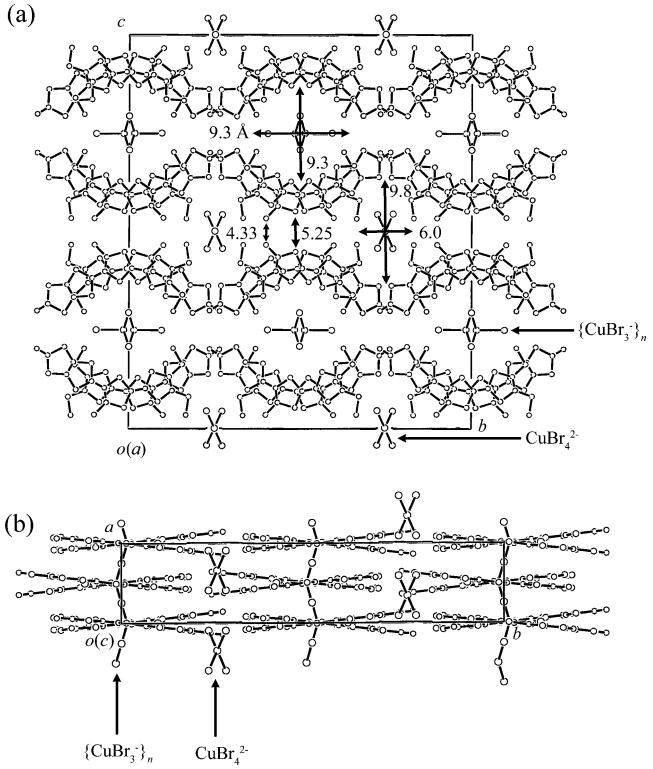

Figure 3. Crystal structure of $\mathbf{1}_4$·$CuBr_4$·$2CuBr_3$: views projected down along the (a) *a* and (b) *c* axes.

of two CH_3S groups, and at the exo C═C bond connected with the III or III/IV ring. The III and III/IV rings have also small AO coefficients at the two S atoms and the one C atom of the C═C bond. However, the AO coefficients are negligibly small at the C and S atoms of the C═S group and also at all the atoms of the dithiocarbonato group. Accordingly, **1** is indeed a unique donor molecule with a highly planar, but largely bent molecular skeleton as well as with a strong electron-donating ability comparable to that of DMT-TTF.

Crystal Structure of $\mathbf{1}_4$·$CuBr_4$·$2CuBr_3$ and Molecular Structures of $CuBr_4^{2-}$ Ion and $\{CuBr_3^-\}_n$. The top and side views of the crystal structure of $\mathbf{1}_4$·$CuBr_4$·$2CuBr_3$ are shown in Figure 3a,b. As is obvious from the figure, a unique framework composed of **1** molecules is formed, which possesses two different shapes of channels included by a one-dimensional array of $CuBr_4^{2-}$ ions and $\{CuBr_3^-\}_n$, respectively.

The crystal of $\mathbf{1}_4$·$CuBr_4$·$2CuBr_3$ involves only one crystallographically independent **1** molecule, whose molecular structure is shown in Figure 4. The molecular skeleton composed of rings I−IV is almost planar, as is obvious from very small dihedral angles (4.0, 1.9, and 0.7°) between I and II, between II and III, and between III and IV, respectively. In addition, the two CH_3S S atoms are also located in the I plane, and the two CH_3S C atoms are apart only by 0.01 and 0.16 Å from the plane, showing that the whole molecule including the two CH_3S groups has a high planarity in contrast to neutral **1a**,**b** molecules. The distance of the C═C bond in the central tetrathiaethylene moiety is 1.39 Å, which becomes longer by 0.05−0.06 Å as compared with

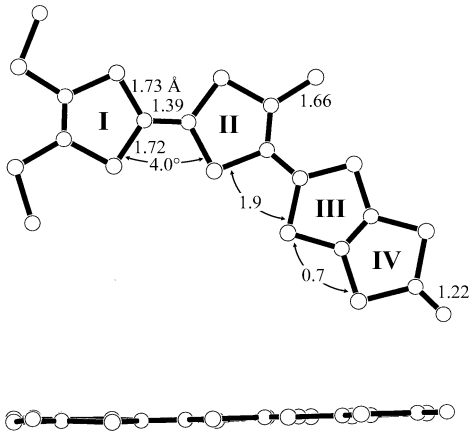

Figure 4. Molecular structure of **1** molecule in $\mathbf{1}_4$·$CuBr_4$·$2CuBr_3$.

those (1.33 and 1.34 Å) of **1a**,**b**, while the C−S bonds (1.72 and 1.73 Å) have shorter distances than the corresponding bond distances (1.77 Å) of the neutral molecules. The comparison of these bond distances between the **1** molecule in $\mathbf{1}_4$·$CuBr_4$·$2CuBr_3$ and the neutral molecules suggests that the **1** molecule in $\mathbf{1}_4$·$CuBr_4$·$2CuBr_3$ is undoubtedly positively charged and can be represented by a resonance structure as shown below. The C═S and C═O bond distances are almost the same as those of **1a**,**b**, 1.66 and 1.22 Å, respectively.

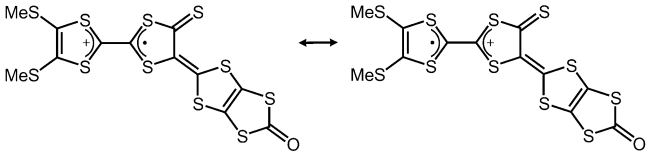

The **1** molecules (**A** (**A**″) and **A**′) are stacked, making the molecular skeletons invert and slide to the right and left sides alternately, but making the C═S groups align in the same direction to form a one-dimensional column like a half-cut pipe, which is tilted by an angle of 6.3° to the right or left direction from the *a* axis (see Figure 5a). The column has two different interplanar distances of 3.40 and 3.51 Å between **A** and **A**′ and between **A**′ and **A**″, respectively, whose overlaps are very slightly different from each other (see Figure 5b,c). Such columns are arranged along the *b* axis, making the arcs align in the same direction, while along the *c* axis changing the arc direction alternately. However, there is almost no contact between the neighboring columns along the *b* axis (only very small overlap between C═O groups of the dithiocarbonato groups) and also along the *c* axis (the distances between the S atoms of the C═S groups and between the S atoms of the tetrathiaethylene moiety are short, 4.33 and 5.25 Å, which are fairly longer than 3.70 Å of the van der Waals' contact distance[29]). Accordingly, it should be noted that the **1** column has a markedly different structure from familiar columns obtained so far by π electron donors with a straight molecular skeleton, in which strong two- and/or three-dimensional interactions between the

(29) Pauling, L. *The Nature of the Chemical Bond*, 3rd ed.; Cornell University Press: Ithaca, New York, 1960.

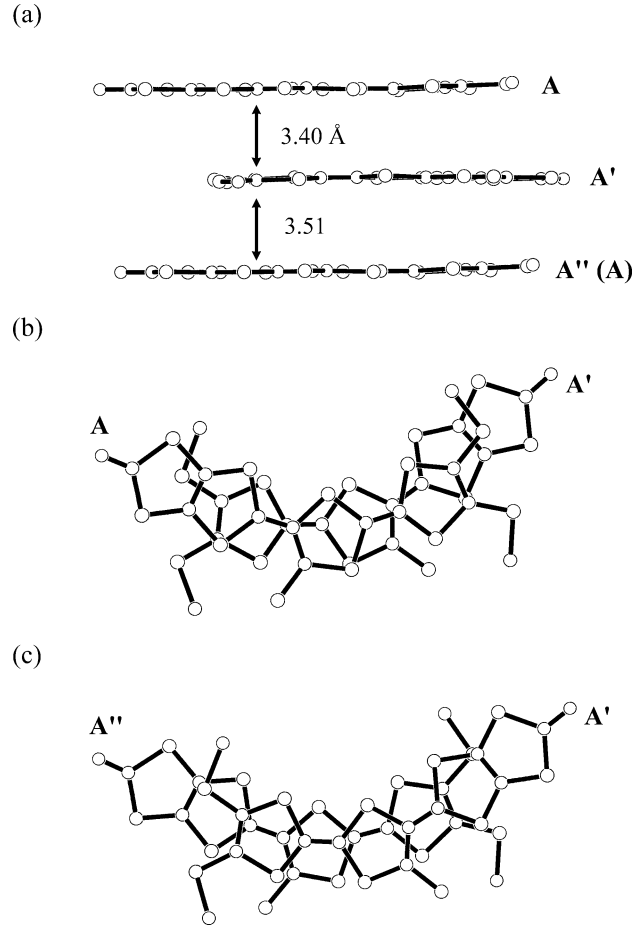

Figure 5. Stacking structure of **1** molecules (**A**, **A**′, and **A**″): (a) side view; overlaps (b) between **A** and **A**′ and (c) between **A**′ and **A**″.

neighboring columns can usually occur. As the result of column arrangement as above, two different kinds of channels are produced, whose sections are oval-shaped (the long and short axes are calculated as interatomic distances between the S atoms in the face-to-face IV rings and between the face-to-face CH_3S C atoms, respectively, and are ca. 9.8 and ca. 6.0 Å) and circle-shaped (the diameter is ca. 9.3 Å, which corresponds to an interatomic distance between the face-to-face CH_3S C atoms), respectively. The four columns forming the oval-shaped channel are all tilted in the same direction from the *a* axis, while the two columns forming the circle-shaped channel are in the reverse direction to each other.

In the oval-shaped channel each of the $CuBr_4^{2-}$ ions is located in the central position surrounded by the eight molecules of **A**, **A**′, and **A**″ and aligned straightly, as shown in Figure 6a,b. The Br···Br distances between the neighboring $CuBr_4^{2-}$ ions are 3.78 and 4.78 Å, and in particular the former value is shorter than the distance (3.90 Å) of the corresponding van der Waals' contact.[29] The four CH_3 groups are thrusted out toward the channel as well as several S atoms of the molecular skeleton, and C═S and CH_3S groups are located around there, so that the channel space has a special environment for the accommodation of the $CuBr_4^{2-}$ ion. The coordination geometry of Br atoms around the Cu atom is markedly different from those of the $CuBr_4^{2-}$ ions in the

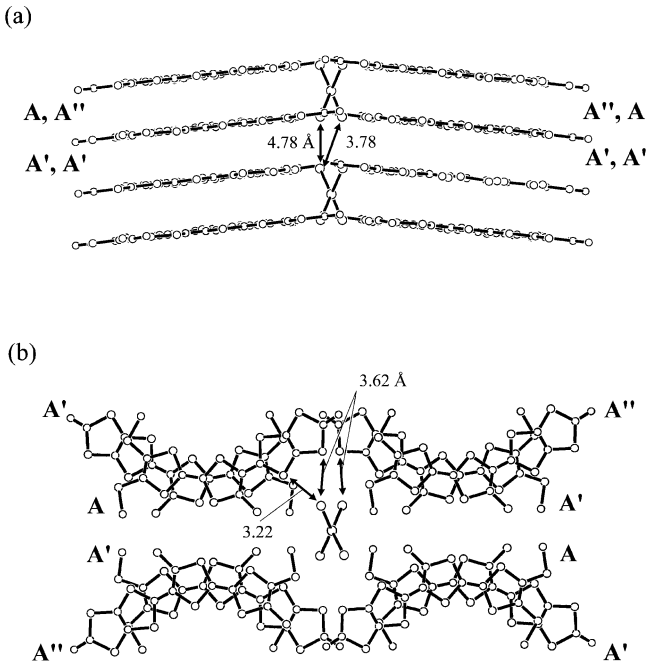

Figure 6. $CuBr_4^{2-}$ ion included in the oval-shaped channel: (a) side view; (b) top view.

unforced environment. Thus, in the present $CuBr_4^{2-}$ ion the Br−Cu−Br bond angles are 92.2, 92.2, 98.1, 98.1, 145.2, and 145.2°, of which 145.2° is larger than the usual values, but fairly small as compared with the values observed in several $CuBr_4^{2-}$ salts, in particular 179.2° in the 3-picolinium ylammonium $CuBr_4^{2-}$ salt.[30] In addition, the Cu−Br bond distances are all 2.51 Å, which is also fairly longer than the usual values but not without precedent (for example, 2.49 Å in the above $CuBr_4^{2-}$ salt).[30] The unusually large Br−Cu−Br bond angle and long Cu−Br bond distance might be due to the abnormal coordination geometry of Br atoms around the Cu atom caused by steric repulsion between the Br atoms of $CuBr_4^{2-}$ ion and CH_3 groups thrust out toward the channel and also probably due to significant interaction between the Br atoms of $CuBr_4^{2-}$ ion and the S atoms of the tetrathiaethylene and dithiocarbonato groups in particular, as shown in Figure 6b, in which Br···S contacts with shorter distances than the sum (3.80 Å) of van der Waals' radii of Br and S atoms[29] are depicted.

On the other hand, $\{CuBr_3^-\}_n$ is included in the circle-shaped channel. As shown in Figure 7a,b, $\{CuBr_3^-\}_n$ consists of a bibromide-bridged linear chain of $CuBr_3^-$ ions, each of which has a distorted square-pyramidal geometry at the Cu atom, as seen from the different angles of the same 90.5° for the Br(2)−Cu(1)−Br(3′) and Br(3)−Cu(1)−Br(2′) bonds, and of the same 84.7° for the Br(2)−Cu(1)−Br(3) and Br(2′)−Cu(1)−Br(3′) bonds, and from almost the same angles of 101.7° for the Br(1)−Cu(1)−Br(2), Br(1)−Cu(1)−Br(3), Br(1)−Cu(1)−Br(2′), and Br(1)−Cu(1)−Br(3′) bonds. The apical Cu(1)−Br(1) bond distance is 2.64 Å, which is fairly longer than those (2.44, 2.54, 2.44, and 2.54 Å) of the equatorial Cu(1)−Br(2), Cu(1)−Br(3), Cu(1)−Br(2′), and Cu(1)−Br(3′) bonds involved in the bridge formation. Each

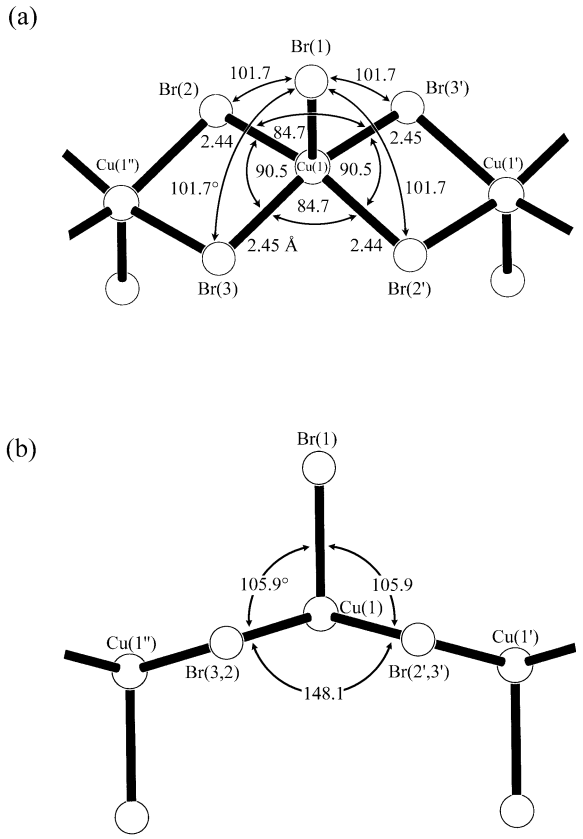

Figure 7. Molecular structure of $\{CuBr_3^-\}_n$ with bond distances (Å) and bond angles (deg): (a) top view; (b) side view.

of the four-membered Cu(1)−Br(2)−Cu(1″)−Br(3) and Cu(1)−Br(2′)−Cu(1′)−Br(3′) rings, etc., is completely planar, as is obvious from the dihedral angle of 180.0° between the two three-membered Br(2)−Cu(1)−Br(3) and Br(2)−Cu(1″)−Br(3) rings and Br(2′)−Cu(1)−Br(3′) and Br(2′)−Cu(1′)−Br(3′) rings, etc. The dihedral angle between the planar four-membered rings is 148.1°.

$\{CuBr_3^-\}_n$ with the edge-sharing of the square pyramids has previously been reported in the cyclohexylammonium salt of $CuBr_3^-$ ion.[31] The X-ray structure analysis of the cyclohexylammonium $CuBr_3^-$ salt was performed, but a satisfactory result on the crystal structure could not be obtained.[32,33] However, the crystals of both a parent non-deuterated and a newly prepared perdueterated cyclohexylammonium salts were solved and refined to 6% by neutron diffraction.[34] In this $\{CuBr_3^-\}_n$ four equatorial Cu−Br bond distances are 2.427, 2.430, 2.454, and 2.459 Å, and the apical Cu−Br bond has a longer distance (2.678 Å). The angles are 86.30, 86.34, 91.86, and 92.24° for the four Br(equatorial)−Cu−Br(equatorial) bonds and 94.27, 95.79, 97.96, and 98.81° for the four Br(equatorial)−Cu−Br(apical) bonds. The two square-pyramidal structures are very similar

(30) Long, G. S.; Wei, M.; Willett, R. D. *Inorg. Chem.* **1997**, *36*, 3102.
(31) Willet, R. D.; Landee, C. P.; Gaura, R. M.; Swank, D. D.; Groenendijk, H. A.; van Duyneveldt, A. J. *J. Magn. Magn. Mater*. **1980**, *15*−*18*, 1055.
(32) Kopinga, K.; Tinus, A. M. C.; de Jonge, W. J. M. *Phys. Rev. B* **1982**, *25*, 4685.
(33) Phaff, A. C.; Swüste, C. H. W.; de Jonge, W. J. M.; Hoogerbeets, R.; van Duyneveld, A. J. *J. Phys. C* **1984**, *17*, 2583.
(34) de Vries, G. C.; Helmholdt, R. B.; Frikkee, E.; Kopinga, K.; de Jonge, W. J. M.; Godefroi, E. F. *J. Phys. Chem. Solids* **1987**, *48*, 803.

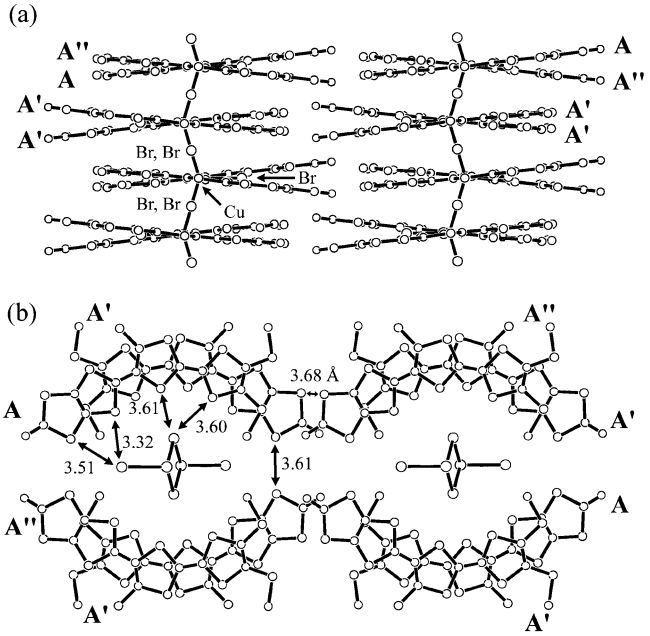

Figure 8. $\{CuBr_3^-\}_n$ included in the circle-shaped channel: (a) side view; (b) top view.

to each other from the comparison of the Cu−Br bond distances and the Br−Cu−Br bond angles between them. Nevertheless, the edge-sharing geometry of the neighboring square pyramids is largely different from that in the present $\{CuBr_3^-\}_n$, as mentioned above. Thus, the dihedral angles between the two three-membered Br−Cu−Br rings are 130.3 and 155.8° for the perdeuterated and nondeuterated cyclohexylammonium $CuBr_3^-$ salts, respectively.

Each of the Cu−Br(apical) bonds in $\{CuBr_3^-\}_n$ lies on the plane of one layer composed of two **1** molecules, while the two equatorial Br atoms are located in the middle between the layers (see Figure 8a,b). There are several close contacts between the Br atoms of each $CuBr_3^-$ ion and the S atoms of four **1** molecules surrounding the $CuBr_3^-$ ion. The Br···S distances (3.32−3.62 Å) fairly shorter than that (3.80 Å) of the corresponding van der Waals' contact[29] can be seen between the Br atoms of $CuBr_3^-$ ion and the S atoms of central tetrathiaethylene and III/IV groups.

Electrical Conducting Property. This single crystal has a needlelike shape with very small sectional area (<0.020 × 0.025 mm^2), so that four electrodes can only be attached to the surface along the long axis, which presumably corresponds to the stacking direction of **1** molecules on the analogy of the needle crystals of **2**, whose molecular stacking axes have distinctly been determined by the four-circle X-ray structure analysis.[34] The electrical conductivity at 300 K was unexpectedly high (2.0×10^{-2} S cm^{-1}), although each of the **1** molecules is completely charged by +1. This might be due to much decrease in the Coulomb repulsion between the positive charges, because the +1 charge is much more extensively distributed on the whole **1** molecule rather than on the tetrathiaethylene moiety as shown above. The electrical conducting behavior of $\mathbf{1}_4{\cdot}CuBr_4{\cdot}2CuBr_3$ is semiconducting in the whole temperature range measured, and the activation energy is fairly large (160 meV). Each of the

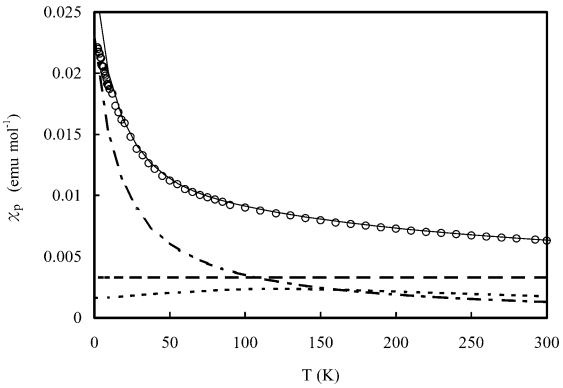

Figure 9. Temperature dependence of χ_p (○) in the temperature range 1.8−300 K for the microcrystals of $\mathbf{1}_4{\cdot}CuBr_4{\cdot}2CuBr_3$. The solid curve (—) was obtained by adding $C = 0.41$, $\Theta = -18$, $J/k_B = -120$, and $\chi_\pi = 3.3 \times 10^{-3}$ to an equation of $\chi_p = \chi(CuBr_4^{2-}) + \chi(\{CuBr_3^-\}_n) + \chi_\pi$, where $\chi(CuBr_4^{2-})$ (− · −) and $\chi(\{CuBr_3^-\}_n)$ (---) are obtained by the Curie−Weiss and Bonner−Fisher expressions, respectively, and χ_π (− − −) is related to the conducting π electrons on the **1**-stacked columns.

1-stacked columns is completely separated from each other, suggesting that this electrical conducting property is actually *one-dimensional*. In addition, since the **1**-stacked columns reside very near the one-dimensional array of the $CuBr_4^{2-}$ ions and $\{CuBr_3^-\}_n$, the as-observed electrical conducting results might be caused by the influence of their magnetic moments.

ESR. In the ESR spectrum of the microcrystals of $\mathbf{1}_4{\cdot}CuBr_4{\cdot}2CuBr_3$ at 300 K one weak and broad (peak-to-peak width, $\Delta H_{pp} = 607$ Oe) doublet signal appeared at $g = 2.0873$. This signal can be readily assigned to be due to the Cu(II) d spins of $CuBr_4^{2-}$ ions and $\{CuBr_3^-\}_n$ from the observed *g*-value.[35] Presumably, the signal with a comparatively weak intensity due to the conducting π spins of **1** molecules is also very broad[36,37] and hidden inside the d signal. With lowering of the temperature from 300 K, the signal intensity increased and the increasing tendency continued until 3 K, the lowest temperature in this measurement. However, there was almost no change in the *g* and ΔH_{pp} values in the temperature range, suggesting that no significant change occurs in both of the interactions between the d spins of $CuBr_4^{2-}$ ions and $\{CuBr_3^-\}_n$.

Magnetic Properties. The temperature dependence of χ_p is shown in Figure 9. The χ_p very slowly increased as the temperature was gradually lowered from 300 K, indicating preferential occurrence of antiferromagnetic interaction in the whole spin system of $\mathbf{1}_4{\cdot}CuBr_4{\cdot}2CuBr_3$. The $\chi_p - T$ data were analyzed by an equation of $\chi_p = \chi(CuBr_4^{2-}) + \chi(\{CuBr_3^-\}_n) + \chi_\pi$, where $\chi(CuBr_4^{2-})$ obeys a Curie−Weiss law with an equation of $\chi(CuBr_4^{2-}) = C/(T - \Theta)$ (*C*, Curie constant; Θ, Weiss temperature); $\chi(\{CuBr_3^-\}_n)$ is analyzed as a Heisenberg chain of $S = 1/2$ spins interacting with a

(35) Iwamatsu, M.; Kominami, T.; Ueda, K.; Sugimoto, T.; Tada, T.; Nishimura, K.-i.; Adachi, T.; Fujita, H.; Guo, F.; Yokogawa, S.; Yoshino, H.; Murata, K.; Shiro. M. *J. Mater. Chem.* **2001**, *11*, 385.
(36) Matsumoto, T.; Kominami, T.; Ueda, K.; Sugimoto, T.; Tada, T.; Yoshino, H.; Murata, K.; Shiro, M.; Negishi, E.; Matsui, H.; Toyota, N.; Endo, S.; Takahashi, K. *J. Solid State Chem.* **2002**, *168*, 408.
(37) Matsumoto, T.; Kominami, T.; Ueda, K.; Sugimoto, T.; Tada, T.; Noguchi, S.; Yoshino, H.; Murata, K.; Shiro, M.; Negishi, E.; Toyota, N.; Endo, S.; Takahashi, K. *Inorg. Chem.* **2002**, *41*, 4763.

coupling constant J, and χ_π is almost a temperature-independent χ_p related to the conducting π electrons on the **1**-stacked columns. Note that in the Curie−Weiss and the Bonner−Fisher expressions[38] the spin amount of $CuBr_3^-$ ions is twice as much as that of $CuBr_4^{2-}$ ions, since one $CuBr_4^{2-}$ ion and two $CuBr_3^-$ ions are involved per formula unit of $\mathbf{1}_4$·$CuBr_4$·$2CuBr_3$ and their average g values are 2.0873, as obtained from the ESR measurement. The fitting to the observed data was performed by choosing appropriate C, Θ, J, and χ_π, and the best result was obtained by the following values: $C = 0.41$ emu K mol^{-1}; $\Theta = -18$ K; $J/k_B = -120$ K; $\chi_\pi = 3.3 \times 10^{-3}$ emu mol^{-1}. Judging from the so-obtained Θ and J, the interaction between the d spins of $CuBr_4^{2-}$ ions is antiferromagnetic and the magnitude is as usual small, while the d spins of $CuBr_3^-$ ions in $\{CuBr_3^-\}_n$ are subject to very strong and antiferromagnetic interactions, which is in marked contrast to a moderately ferromagnetic interaction with $J/k_B = +(55 \pm 5)$ K in the $\{CuBr_3^-\}_n$ in the cyclohexylammonium $CuBr_3^-$ salt.[32,33]

As mentioned above, the two $\{CuBr_3^-\}_n$'s have very similar square pyramids at the Cu atom. However, the edge-sharing geometries of the neighboring square pyramids are different from each other. Thus, in the present $\{CuBr_3^-\}_n$ each of the four-membered Cu−Br−Cu−Br rings is completely planar, while nonplanar and puckered in the $\{CuBr_3^-\}_n$ in the cyclohexylammonium salt. As a matter of course it is conceivable that this difference in the chain structures between the two $\{CuBr_3^-\}_n$'s is responsible for their markedly different interactions between the Cu(II) d spins. The MO calculation was performed to make sure of whether antiferromagnetic interaction is also predicted theoretically in the present $\{CuBr_3^-\}_n$. The Cu_2Br_8 moiety involving the two Cu atoms can be regarded as a component unit to investigate the interaction between the Cu(II) d spins in the present $\{CuBr_3^-\}_n$, so that the J value was calculated by using a UCCSD(T) method with the highest level of accuracy in the MO calculation of open-shell systems at the present time[39] and the atomic coordinates of the Cu_2Br_8 moiety obtained from the crystal structure data. The moderate and positive value of +36 K was obtained, suggesting that like the Cu_2Br_8 moiety the present $\{CuBr_3^-\}_n$ has also a preference for a ferromagnetic interaction between the two Cu(II) d spins. This discrepancy between the theoretical prediction and the observed result gives a possibility that the spin interaction was changed from ferromagnetic to antiferromagnetic by a significant interaction between the $\{CuBr_3^-\}_n$ and the **1**-stacked π conducting columns, which have very close contacts with each other.

(38) Bonner, J. C.; Fisher, M. E. *Phys. Rev. A* **1964**, *135*, 640.
(39) *Gaussian 98, Revision A. 11*; Gaussian Inc.: Pittsburgh, PA, Philadelphia, PA, 2001.

Concluding Remarks

In the CT salts of familiar donor molecules such as TTF and TSF derivatives with a planar and straight molecular skeleton, the crystal structures are alternately stacked by each of the donor molecule and counteranion layers. Nevertheless, in the case of **1** with a planar but largely bent molecular skeleton, as observed by $\mathbf{1}_4$·$CuBr_4$·$2CuBr_3$, the **1**-stacked columns with a half-cut pipelike shape are arranged to turn the concave or convex faces to the same direction with each other, so that two different kinds of channels are formed, in which the $CuBr_4^{2-}$ and $CuBr_3^-$ counteranions are included as a one-dimensional array and as a one-dimensional chain with a square-pyramidal structure, respectively. Since there is only a very weak contact between the neighboring **1**-stacked columns, this π conducting column is essentially *one-dimensional*. Consequently, $\mathbf{1}_4$·$CuBr_4$·$2CuBr_3$ is an unprecedented molecular π/d system containing both one-dimensional conducting π electrons and localized d spins in the one-dimensional array and chain, so that it is very interesting in comparing electrical conducting/magnetic properties and the π/d interaction mode of this molecular π/d system with those of two- and three-dimensional molecular π/d systems obtained so far.

The present $\{CuBr_3^-\}_n$ exhibited a unusual interaction between the Cu(II) d spins, which is remarkably different from the theoretical prediction. It is very likely that the significant interaction between the $\{CuBr_3^-\}_n$ and **1**-stacked π conducting columns actually occurs, bringing about the marked change from ferromagnetic to antiferromagnetic interaction. In correspondence to this magnetic change, the electrical conducting properties on the **1**-stacked π conducting columns might be also influenced. We are now investigating the electrical conducting and magnetic properties in more detail.

Acknowledgment. This work was supported in part by a Grant-in-Aid for Scientific Research on Priority Areas (B) (No. 11224209) from the Ministry of Education, Culture, Sports, Science, and Technology of Japan. We thank Dr. H. Fujiwara and Prof. H. Kobayashi (Institute for Molecular Science) for ESR measurement and Prof. K. Mukai (Ehime University) for discussion on the magnetic measurement data.

Supporting Information Available: X-ray crystallographic data in CIF format for **1** and $\mathbf{1}_4$·$CuBr_4$·$2CuBr_3$. This material is available free of charge via the Internet at http://pubs.acs.org.

IC0300971